

# Synthesis and structural characterization of a magnesium phthalocyanine(3–) anion

Edwin W.Y. Wong and Daniel B. Leznoff\*<sup>◇</sup>

Department of Chemistry, Simon Fraser University, 8888 University Drive, Burnaby BC, V5A 1S6, Canada

Received 1 October 2011

Accepted 19 October 2011

**ABSTRACT:** The reduction of magnesium phthalocyanine (MgPc) with 2.2 equivalents of potassium graphite in 1,2-dimethoxyethane (DME) gives  $[K_2(DME)_4]PcMg(OH)$  (**1**) in 67% yield. Compound **1** was structurally characterized using single crystal X-ray crystallography and was found to be a monomeric, heterometallic complex consisting of a  $\mu_3$ -OH ligand that bridges a  $[Mg^{II}Pc^{3-}]$  anion to two potassium cations solvated by four DME molecules. An absorption spectrum of **1** confirms the Pc ligand is singly reduced and has a 3– charge. The solid-state structure of **1** does not indicate breaking of the aromaticity of the Pc ligand. Compound **1** is only the second  $Pc^{3-}$  complex and the first reduced MgPc to be isolated and structurally characterized.

**KEYWORDS:** magnesium, phthalocyanine, reduction, anion, X-ray crystal structure.

## INTRODUCTION

Investigation into the spectroscopic and redox properties of metallophthalocyanines (MPcs) continue to be active areas of research [1–8]. MPc complexes can be successively reduced using chemical, electrochemical, or photochemical methods to give rise to species containing reduced  $Pc^{3-}$ ,  $Pc^{4-}$ ,  $Pc^{5-}$ , or  $Pc^{6-}$  ligands, which drastically affect the spectral properties of the complexes [9]. The electronic absorption spectra of these ring-reduced MPc anions have been studied extensively. Much of this work has focused on main group MPcs (M = Mg, Al, Ge, Zn) since the unvarying oxidation state of the main group metal simplifies the determination of the charge on the Pc ligand. Indeed, the first report of an absorption spectrum of a reduced MPc was of a chemically reduced MgPc [10]. The spectra of the whole series of chemically reduced MgPc anions was reported again by Clack and Yandle [9]. Magnetic circular dichroism (MCD) spectroscopy has been used in conjunction with absorption spectroscopy to gather additional information on the electronic structure of

MgPc reduced by chemical methods [11], as well as electrochemical methods [12]. However, no reduced MgPc species has ever been isolated or structurally characterized.

The anions of ZnPc have also been comprehensively studied *in situ*. The absorption spectra of chemically [9], electrochemically [9, 13–16], and photochemically [17] reduced ZnPc have been reported along with the MCD spectra of photochemically [16, 17] and electrochemically [14] reduced ZnPc. While MgPc and ZnPc are the most commonly investigated main group MPcs, the absorption spectra of chemically reduced AlPc [9, 18, 19] and GePc [20] species have also been reported.

In spite of the additional challenge of variable oxidation states at the metal centre, reduced transition metal Pcs have also been investigated. The absorption spectra of chemically reduced Mn, Fe, Ni [9], and Nb [21] Pcs and electrochemically reduced Fe [15, 22], Co [15, 23, 24], Ni [23], and Cu [13, 23], Pcs are available. The absorption spectra of some rare examples of electrochemically reduced actinide Pcs containing U and Th are also known [25].

In spite of this body of work on the electronic absorption spectra of ring-reduced MPcs, these species are usually generated and characterized *in situ* and have only very rarely been isolated for structural characterization,

<sup>◇</sup>SPP full member in good standing

\*Correspondence to: Daniel B. Leznoff, email: [dleznoff@sfu.ca](mailto:dleznoff@sfu.ca), tel: +1 778-782-4887, fax: +1 778-782-3765

even though structural information would be useful for interpreting the spectroscopic data [26]. This is likely due to the extreme sensitivity of these complexes, which can only be isolated under the *rigorous* exclusion of air and moisture [27]. Although the isolation of a series of reduced first-row transition metal and main group element Pcs was reported [27], none of these compounds were ever structurally characterized.

Indeed, only five of these elusive compounds have been isolated and structurally characterized to our knowledge. Specifically, reduced FePc complexes with the formulas  $K([2.2.2]\text{cryptand})\text{FePc}$  and  $\text{Li}_2(\text{THF})(18\text{-crown-6})_2\text{FePc}$  (THF = tetrahydrofuran) have been structurally characterized [28]. The single crystal X-ray structures of  $\text{Al}^{\text{III}}\text{Pc}^{3-}(\text{anisole})_2$  [18] and  $\text{Ge}^{\text{IV}}\text{Pc}^+(\text{pyridine})_2$  have also been reported [20]. We recently described the structural and electronic characterization of a reduced NbPc species,  $\text{K}_2\text{Nb}^{\text{IV}}\text{Pc}^+\text{O}\cdot 5\text{DME}$  (DME = 1,2-dimethoxyethane) [21]. Of the five reported structures, all feature nearly planar Pc ligands except for  $\text{K}_2\text{Nb}^{\text{IV}}\text{Pc}^+\text{O}\cdot 5\text{DME}$ , which has a saddle-shaped Pc ligand [21].

The addition of electrons to the aromatic  $18\pi$ -electron circuit of the Pc ligand *via* reduction is expected to disrupt its aromaticity [20]. The effects of MPc reduction are most dramatically seen in the doubly reduced  $\text{Ge}^{\text{IV}}\text{Pc}^+(\text{pyridine})_2$  and  $\text{K}_2\text{Nb}^{\text{IV}}\text{Pc}^+\text{O}\cdot 5\text{DME}$  systems in the form of bond localization, which manifests itself in the form of alternating short and long bonds around the Pc ligand [20, 21]. Interestingly, in both compounds, the bond-length alternation is seen in only two of the four benzo groups situated *trans* to each other [20, 21]. This bonding pattern is consistent with a simple valence-bond model of the Pc ligand, where two of the four opposing benzo moieties are expected to be delocalized and the remaining two are expected to show localized bonding [20]. There is evidence of antiaromaticity in the  $^1\text{H}$  NMR spectrum of the  $20\pi$ -electron  $\text{Ge}^{\text{IV}}\text{Pc}^+$  system, in which resonances are shifted from their expected positions by a strong paratropic ring current [20]. Nucleus independent shift calculations also predicted the antiaromatic character of  $\text{Ge}^{\text{IV}}\text{Pc}^+$  [20].

In the case of  $\text{MPc}^{3-}$  complexes, the predicted loss of aromaticity does not manifest itself significantly in the structural data. For instance, there is little to no bond-length alternation observed in  $\text{Al}^{\text{III}}\text{Pc}^{3-}(\text{anisole})_2$  in spite of the fact that DFT calculations predict that it should be present [18]. Conversely, bond-length alternation is seen in a similar singly reduced  $\text{Al}(\text{TPP})(\text{THF})_2$  complex (TPP = tetraphenylporphyrin) [18].

Our previous success at isolating and structurally characterizing  $\text{K}_2\text{Nb}^{\text{IV}}\text{Pc}^+\text{O}\cdot 5\text{DME}$  [21] motivated us to examine the more commonly studied ring-reduced MPcs, such as MgPc in a similar fashion. Herein, we report the first isolation of a reduced MgPc system and only the second  $\text{Pc}^{3-}$  anion to be structurally characterized, namely  $\text{Mg}^{\text{II}}\text{Pc}^{3-}$ .

## RESULTS AND DISCUSSION

### Synthesis and structure

The addition of 2.2 equivalents of potassium graphite ( $\text{KC}_8$ ) to a stirred mixture of MgPc in DME results in an immediate reaction to give a dark purple mixture. Filtration of the reaction mixture through a pad of Celite on a frit filter initially resulted in decomposition of the purple product into a blue-green material due to the extreme sensitivity of the purple product. After this initial decomposition, the remaining purple filtrate was collected since it retained its original colour as it passed through the frit filter. A dark purple powder of  $[\text{K}_2(\text{DME})_4]\text{PcMg}(\text{OH})$  (**1**) was obtained in 67% yield after removal of the solvent under reduced pressure.

Elemental analysis (C, H, N) of **1** is consistent with an empirical formula of  $[\text{K}_2(\text{DME})_4]\text{PcMg}(\text{OH})$ . A mass spectrum of **1** could not be obtained because **1** decomposes immediately upon exposure to even small traces of oxygen. However, a MALDI-TOF mass spectrum of a sample of **1** exposed to air reveals that **1** decomposes to MgPc ( $m/z = 536.1$ , calcd. for  $\text{C}_{32}\text{H}_{16}\text{N}_8\text{Mg} = 536.1$   $[\text{M}^+]$ ). As further confirmation, the absorption spectrum of the decomposition product is nearly identical with the spectrum of MgPc in DME. Extraction of the decomposition products of **1** with water yields a basic solution, which is consistent with the presence of KOH, the other expected decomposition product. A controlled oxidation of **1** with ferrocenium tetrafluoroborate in an inert atmosphere also yields MgPc and KOH.

Purple crystals suitable for single crystal X-ray diffraction were grown by layering hexanes over a DME solution of **1**. At some point in the reaction, the reactants or products were inadvertently exposed to traces of oxygen and moisture, this being the source of the hydroxide ligand. Nevertheless, regardless of the details of its isolation, the structure of compound **1** is of interest due to the near absence of structurally characterized  $\text{MPc}^{3-}$  complexes in the literature.

Compound **1** is a monomeric, heterometallic complex consisting of a  $\mu_3$ -OH ligand that bridges a  $[\text{Mg}^{\text{II}}\text{Pc}^{3-}]$  anion and two potassium cations (Fig. 1), which are solvated by four DME molecules. The crystal structure of **1** shows that it is highly distorted in the solid state and no longer contains an axis of symmetry. The Mg centre is 5-coordinate with a distorted square-pyramidal geometry consisting of four basal isoindole N-atoms and the apical  $\mu_3$ -O-atom of the hydroxide ligand. The average Mg to basal N distance in **1** is 2.072(2) Å, whereas the average for MgPc (X-ray data collected at 120 K) is slightly shorter (2.048 Å) [29]. Correspondingly, the distance of the Mg centre to the  $\text{PcN}_4$  mean plane in **1** (0.595 Å) is slightly greater than in MgPc (0.557 Å) [29].

The hydroxide oxygen atom, O1, is not situated directly above Mg1 but is angled back towards the potassium cations. This is evidenced by the asymmetry observed

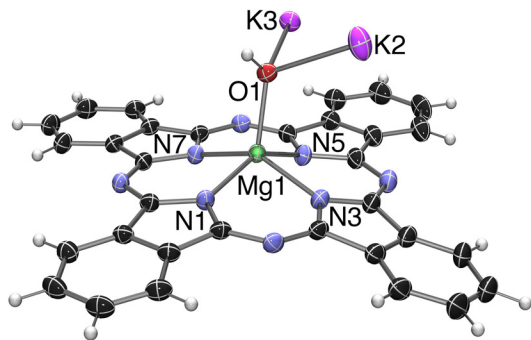


**Fig. 1.** Molecular structure of  $[K_2(DME)_4]PcMg(OH)$  (**1**) with potassium-bound DME molecules removed for clarity. Thermal ellipsoids are set at 30% probability

in the pairs of opposing isoindole  $NX-Mg1-O1$  ( $X = 1$  and  $5, 3$  and  $7$ ) bond angles. The  $N3-$  and  $N7-Mg1-O1$  pair of angles are essentially the same at  $106.66(11)^\circ$  and  $106.00(11)^\circ$ , respectively, but the  $N1-$  and  $N5-Mg1-O1$  pair of angles are quite different at  $114.73(11)^\circ$  and  $99.06(11)^\circ$ , respectively.  $O1$  of the  $\mu_3$ -OH ligand adopts a distorted tetrahedral geometry. Previously, a  $\mu_3$ -OH was reported to bridge two potassium atoms to a transition metal atom in a bis(imino)pyridine iron dimer [30] and in a ruthenium complex [31]. The  $K2-O1$  and  $K3-O1$  bond lengths of  $2.644(2)$  Å and  $2.638(2)$  Å, respectively, are slightly shorter than previously reported  $K-O$  distances, which average  $2.716(1)$  Å [30, 31].

The asymmetry of **1** also manifests itself in the position of the potassium cations.  $K2$  lies  $3.758$  Å above the  $Pc-C_8N_8$  mean plane whereas  $K3$  lies much closer to the  $Pc$  ligand at only  $2.989$  Å. There appear to be significant interactions between  $K3$  and  $C23, C24, N5,$  and  $N6$  of the  $Pc$  ligand judging by their relatively close contacts. However, this does not appear to cause any localization of the bonds within the  $Pc$  ligand since no bond length-alternation is observed in the region of the  $Pc$  ligand near  $K3$ .

The  $Mg1-O1$  bond distance ( $1.948(2)$  Å) is shorter than reported  $Mg-O$  distances for terminal  $Mg-OH$  bonds, which range from  $2.073(3)$  to  $2.199(3)$  Å [32]. However, a shorter  $Mg-O$  distance of  $1.985(6)$  Å has been reported for a  $\mu_3$ -OH that bridges between  $Mg$  and two  $Li$  centres, which is more in line with the  $Mg1-O1$  bond distance observed in **1** [33].

The nature of the  $Pc$  aromaticity after reduction is of interest, but lack of structural information on reduced MPcs [34] has limited the discussion of this topic. Therefore, the conformation of bond distances in the  $Pc$  ligand were examined closely for signs of loss of aromaticity or the presence of anti-aromaticity. The  $Pc$  ligand in **1** is distorted, with the two isoindole moieties on the same side as  $K3$  being relatively flat whereas the isoindoles on the  $K2$  side point downward away from  $K2$ . The dihedral angles between the  $C_8N_8$  mean plane and the  $N5$  and  $N7$  isoindole moieties on the  $K3$  side are  $2.12^\circ$  and  $4.55^\circ$ , respectively, while the dihedral angles between the

$C_8N_8$  mean plane and the  $N1$  and  $N3$  isoindole moieties are much greater at  $9.36^\circ$  and  $12.13^\circ$ , respectively. It is difficult to compare the conformation of the  $Pc$  ligand in **1** to the published structures of  $MgPc$  [29, 35] since disorder of the  $Mg$  centre in the neutral  $MgPc$  structure limits the accuracy of the metrical parameters of the  $Pc$  ligand. A survey of the high quality, ( $R \leq 0.05$ ) low temperature single crystal X-ray structures of  $(L)MgPc$  [36, 37] (where  $L = H_2O$  or  $MeOH$ ) suggests that the  $Pc$  ligand in  $MgPc$  can vary from distorted to nearly planar conformations, which also makes it difficult to compare the conformation of the  $Pc^{3-}$  ligand in **1** to the published structures containing a  $Pc^{2-}$  ligand.

To our knowledge, the only other structurally characterized  $Pc^{3-}$  compound is  $Al^{III}Pc^{3-}(\text{anisole})_2$  (**2**) [18]. In contrast to **1**, **2** is nearly flat and the largest dihedral angle between the  $C_8N_8$  mean plane and an isoindole moiety is  $3.75^\circ$ . There is no strong evidence for breaking of the aromaticity of the  $Pc$  ligand in the form of bond localization in either **1** or **2**, although DFT calculations on **2** predict that it should occur at the  $N_{meso}-C$  bonds [18]. There is some slight bond localization in the form of bond-length alternation in the benzo moieties of the  $Pc$  ligand observed in **2**, but the differences in adjacent  $C-C$  bonds range from statistically insignificant ( $0.003(3)$  Å) to  $0.028(4)$  Å and the difference in length between short and long  $C-C$  bonds is not consistent throughout the  $Pc$  ligand.

With this in mind, the DFT geometry optimized structure (B3LYP/6-31G\*) of  $[MgPc(OH)]^{2-}$  was calculated and it predicts that there should be a pattern of alternating short and long  $N_{meso}-C$  bonds in the  $Pc$  ligand with an average difference of  $0.036$  Å, similar to the difference of  $0.037$  Å calculated for **2** [18]. In **1**, the experimental difference between adjacent  $N_{meso}-C$  bonds only ranges from  $0.018(6)$  to  $0.010(6)$  Å. This discrepancy was also observed for **2**. It is interesting to contrast the structures of  $Pc^{3-}$  ligands with those of  $Pc^{4-}$  ligands. In the case of the two structurally characterized  $Pc^{4-}$  complexes [20, 21], bond-length alternation is clearly observed (*vide supra*).

### Absorption spectroscopy of **1**

The most intense absorption band for MPcs (the Q-band) arises from a ligand-based  $\pi-\pi^*$  transition, which generally lies around  $670$  nm and does not change greatly with varying metal centres [38]. However, oxidation or reduction of the  $Pc$  ligand in a  $MPc$  complex changes the spectrum significantly, where each  $Pc$  charge state has a distinct absorption spectrum [38, 39]. The absorption spectra of reduced  $MgPc$  anions *in situ* have been reported previously [9, 10] and can be compared with the spectrum of **1** to determine the charge of the  $Pc$  ligand. An absorption spectrum of crystals of **1** dissolved in DME (Fig. 2) correspond well with the published spectrum of  $[Mg^{II}Pc^{3-}]$  in THF and, therefore, the  $Pc$

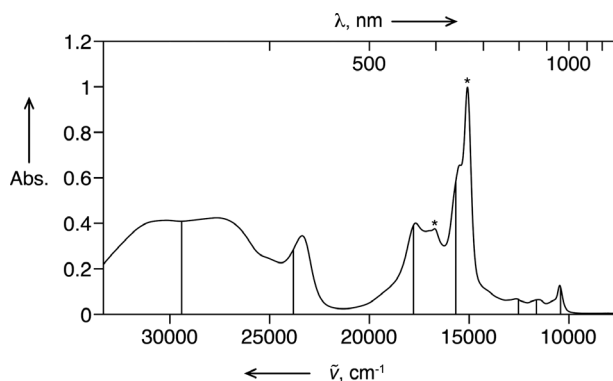


**Fig. 2.** Absorption spectrum of **1** in DME. Vertical bars represent the reported absorptions of  $\text{Mg}^{\text{II}}\text{Pc}^{3-}$  in THF with arbitrary intensities matched to that of the experimental spectrum [9] (\* denote absorptions due to oxidation of **1**)

ligand in **1** has a -3 charge [9]. The -3 charge of the Pc ligand in **1** is also consistent with its molecular formula since the sum of the charge on the remaining ions ( $\text{Mg}^{2+}$ ,  $2 \times \text{K}^+$ ,  $\text{OH}^-$ ) is +3. Compound **1** is extremely unstable with respect to oxidation of the reduced  $\text{Pc}^{3-}$  ligand and it was not possible to obtain a spectrum unobscured by the Q-band of oxidized **1**, which is presumably a  $\text{Pc}^{2-}$  species.

### Insights into the reaction

The mechanism for the formation of **1** is not clear since it would be expected that the addition of 2.2 equivalents of  $\text{KC}_8$  to  $\text{MgPc}$  would result in a  $\text{Mg}^{\text{II}}\text{Pc}^{4-}$  product rather than the  $\text{Mg}^{\text{II}}\text{Pc}^{3-}$  product, **1**, that was obtained. There are two possibilities: (a) that a  $\text{Pc}^{4-}$  product was never formed or (b) that a  $\text{Pc}^{4-}$  formed initially and was subsequently oxidized to the  $\text{Pc}^{3-}$  product **1** that was isolated.

To examine this, the reduction of  $\text{MgPc}$  with  $\text{KC}_8$  was repeated in DME that was degassed using four freeze-pump-thaw cycles, thereby further minimizing any possible immediate oxidation of the products. An absorption spectrum of an aliquot of the reaction mixture was recorded and, in comparison with the spectrum of **1**, the presence of an additional distinct absorption attributable to  $\text{Mg}^{\text{II}}\text{Pc}^{4-}$  at 520 nm [9] appears to indicate that a mixture of  $\text{Mg}^{\text{II}}\text{Pc}^{4-}$  and  $\text{Mg}^{\text{II}}\text{Pc}^{3-}$  products are present in the reaction (Fig. 3), therefore, a  $\text{Pc}^{4-}$  product is initially being produced. It is unclear whether **1** results from the oxidation of the initial  $\text{Pc}^{4-}$  product or whether the  $\text{Pc}^{3-}$  product, **1**, was formed simultaneously in parallel with the  $\text{Pc}^{4-}$  product. In the latter case, it is possible that a portion of the  $\text{KC}_8$  reacts with trace moisture present in the reaction mixture (despite our efforts to exclude moisture) to form potassium hydroxide, which is then incorporated into **1**, rather than all of the  $\text{KC}_8$  acting to reduce the  $\text{MgPc}$  starting material. This is only one possibility of many and due to the inherent reactivity and extreme air and moisture sensitivity of these reduced MPcs it is difficult to determine the exact sequence of events that leads to the formation of **1**.

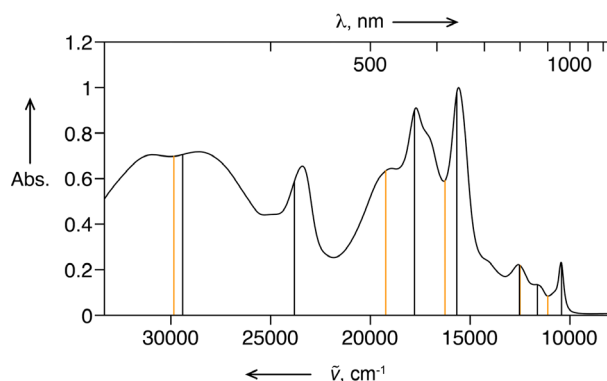


**Fig. 3.** Absorption spectrum of an aliquot of the reaction between  $\text{MgPc}$  and 2.2 equivalents of  $\text{KC}_8$  in DME. Vertical bars represent the reported absorptions of  $\text{Mg}^{\text{II}}\text{Pc}^{3-}$  [9] (black) and  $\text{Mg}^{\text{II}}\text{Pc}^{4-}$  [9] (orange) in THF with arbitrary intensities matched to that of the experimental spectrum

## EXPERIMENTAL

### General methods and procedures

All manipulations were carried out under an atmosphere of dinitrogen in a MBraun Labmaster 130 glovebox or using standard Schlenk techniques unless otherwise stated. All glassware was rigorously dried overnight at 160 °C and cooled under vacuum before use. Potassium graphite [40] was prepared according to a literature procedure. Magnesium phthalocyanine (TCI America) was dried under vacuum overnight before being transferred into a glovebox for use and storage. 1,2-dimethoxyethane (Certified, Fisher) was distilled under a nitrogen atmosphere from a purple solution of sodium benzophenone ketyl and stored over sodium wire in a glovebox. All other reagents were obtained from commercial sources and used as received.

Electronic absorption spectra were recorded on a Varian Cary 5000 spectrophotometer in a 0.1 cm quartz cell or a 0.1 cm quartz cell equipped with a Kontes PTFE plug, HI-VAC valve for air-sensitive samples.

Elemental analyses (C, H, N) were performed by Mr. Farzad Haftbaradaran at Simon Fraser University on a Carlo Erba EA 1110 CHN elemental analyzer. Samples for elemental analyses were loaded into pre-weighed tin capsules inside a glovebox, sealed by crimping the capsules with tweezers, removed from the glovebox, weighed, and promptly loaded into the analyzer.

MALDI-TOF mass spectrometry experiments were performed on a Bruker Biflex IV equipped with a nitrogen laser. The spectra were acquired by matrix-assisted laser desorption/ionization (MALDI) using trans-2-[3-(4-*tert*-butylphenyl)-2-methyl-2-propenylidene]malononitrile (dctb) as a matrix.

### Synthetic procedures

**Preparation of  $[\text{K}_2(\text{DME})_4]\text{PcMg}(\text{OH})$ .**  $\text{KC}_8$  (0.139 g, 1.03 mmol) was added to a dark blue-green suspension

of MgPc (0.250 g, 0.466 mmol) in approximately 20 mL of DME at room temperature. An immediate colour change to dark purple was observed. The mixture was stirred overnight and filtered through Celite. Initially, the purple reaction mixture turned blue-green upon contact with the frit. The blue-green filtrate was discarded. Filtration of the reaction mixture was continued and the filtrate was collected once it retained the original dark purple color of the reaction mixture. The solvent was removed under reduced pressure and a dark purple solid was collected. Yield 0.309 g (66.9%). Anal. calcd. for  $C_{48}H_{57}K_2MgN_8O_9$ : C, 58.09; H, 5.79; N, 11.29%. Found: C, 58.19; H, 5.74; N 11.21.

Purple crystals suitable for X-ray analysis were grown by layering hexanes onto a DME solution of the product in a capped one dram vial. During the recrystallization process, the atmosphere of the glovebox was contaminated with traces of oxygen and  $H_2O$  (< 10 ppm) over a period of several hours on multiple occasions due to power outages. An absorption spectrum of the crystals was recorded. UV-vis (DME):  $\lambda_{max}$ , nm 956, 869, 791, 663, 646, 598, 565, 428, 362, 331.

The above procedure was repeated with an additional step of degassing the DME solvent by four freeze-pump-thaw cycles prior to use. In this case, the DME was used immediately and was not stored over sodium wire. The graphite was allowed to settle to the bottom of the reaction vessel and an absorption spectrum was taken of a drop of the reaction solution diluted with degassed DME. UV-vis (DME):  $\lambda_{max}$ , nm 958, 857, 794, 642, 565, 528, 427, 350, 323.

### Oxidation of **1**

In a glovebox, a small sample of **1** was dissolved in about 1 mL of DME resulting in a dark blue-purple solution. This solution was taken out of the glovebox and turned dark blue-green immediately upon exposure to air. The solvent was allowed to slowly evaporate to give a mixture of colorless and dark blue-green solids. A sample of the mixture was extracted with a few drops of distilled water and the water was found to be basic using pH paper. UV-vis (DME):  $\lambda_{max}$ , nm 666, 637, 602, 343. MS (MALDI-TOF):  $m/z$  536.1 (calcd. for  $C_{32}N_8H_{16}Mg$ : 536.1 [ $M^+$ ]).

In a glovebox, **1** (0.025 g, 0.025 mmol) was dissolved in about 7 mL of DME resulting in a dark blue-purple solution. Ferrocenium tetrafluoroborate (0.0076 g, 0.028 mmol) was added to the solution of **1** and stirred overnight resulting in a dark blue-green solution. The solution was taken out of the glovebox and the solvent was removed under reduced pressure to give a dark blue-green solid. A sample of the dark blue-green solid was extracted with a few drops of distilled water and the water was found to be basic using pH paper. UV-vis (DME):  $\lambda_{max}$ , nm 667, 638, 603, 344. MS (MALDI-TOF):  $m/z$  535.9 (calcd. for  $C_{32}N_8H_{16}Mg$ : 536.1 [ $M^+$ ]).

### Absorption spectrum of MgPc

An absorption spectrum of MgPc in DME was recorded. UV-vis (DME):  $\lambda_{max}$ , nm 668, 639, 604, 345.

### Single crystal X-ray crystallographic analysis

Crystallographic data and select bond lengths and angles for **1** are listed in Tables 1, 2 and 3, respectively. Data were collected through the SCrALS (Service Crystallography at Advanced Light Source) program at the Small-Crystal Crystallography Beamline 11.3.1 at the Advanced Light Source (ALS), Lawrence Berkeley National Laboratory due to the weakly diffracting nature of the crystals of **1**.

Intensity data were collected at 150 K on a D8 goniostat equipped with a Bruker APEXII CCD detector at Beamline 11.3.1 at the ALS using synchrotron radiation tuned to  $\lambda = 0.77490 \text{ \AA}$ . A series of one second frames measured at  $0.2^\circ$  increments of  $\omega$  were collected to calculate a unit cell. For data collection frames were measured for a duration of one second at  $0.3^\circ$  intervals of  $\omega$  with a maximum  $2\theta$  value of  $\sim 60^\circ$ . The data frames were collected using the program APEX2 and processed using the program SAINT routine within APEX2. The data were corrected for absorption and beam corrections based on the multi-scan technique as implemented in SADABS.

The structures were solved using direct methods (SIR92) [41] and refined by least-squares procedures

**Table 1.** Crystallographic data for  $[K_2(DME)_4]PcMg(OH)$  (**1**)

Empirical formula	$C_{48}H_{57}K_2MgN_8O_9$
Formula weight	992.53
Crystal system	monoclinic
Space group	$P2_1/n$
a, $\text{\AA}$	12.570(3)
b, $\text{\AA}$	20.364(5)
c, $\text{\AA}$	20.163(5)
$\alpha$ , $^\circ$	90
$\beta$ , $^\circ$	105.499(3)
$\gamma$ , $^\circ$	90
V, $\text{\AA}^3$	4974(2)
Z	4
T, K	150
$\rho_{calcd}$ , $\text{g/cm}^3$	1.325
$\mu$ , $\text{mm}^{-1}$	0.266
Unique reflections collected	10239
Observed reflections	6373
R [ $I_0 \geq 3\sigma(I_0)$ ]	0.0643
$R_w$ [ $I_0 \geq 3\sigma(I_0)$ ]	0.0761
Goodness of fit	1.0848

**Table 2.** Selected bond lengths (Å) for [K<sub>2</sub>(DME)<sub>4</sub>]PcMg(OH) (1)

K2–O1	2.644(2)	N8–C1	1.353(4)	C19–C20	1.365(6)
K3–O1	2.638(2)	N8–C32	1.335(4)	C20–C21	1.391(7)
Mg1–O1	1.948(2)	C1–C2	1.457(4)	C21–C22	1.377(6)
Mg1–N1	2.066(3)	C2–C3	1.379(5)	C22–C23	1.383(5)
Mg1–N3	2.078(3)	C2–C7	1.404(5)	C23–C24	1.453(5)
Mg1–N5	2.068(3)	C3–C4	1.390(5)	C25–C26	1.457(5)
Mg1–N7	2.075(3)	C4–C5	1.384(6)	C26–C27	1.393(4)
N1–C1	1.363(4)	C5–C6	1.374(5)	C26–C31	1.404(4)
N1–C8	1.381(4)	C6–C7	1.400(5)	C27–C28	1.371(5)
N2–C8	1.341(4)	C7–C8	1.443(5)	C28–C29	1.394(6)
N2–C9	1.328(5)	C9–C10	1.460(5)	C29–C30	1.386(5)
N3–C9	1.366(4)	C10–C11	1.397(5)	C30–C31	1.387(5)
N3–C16	1.373(4)	C10–C15	1.389(6)	C31–C32	1.465(4)
N4–C16	1.327(5)	C11–C12	1.381(6)	K2–O101	2.808(4)
N4–C17	1.345(5)	C12–C13	1.390(7)	K2–O102	2.830(3)
N5–C17	1.376(4)	C13–C14	1.367(7)	K2–O401	2.763(5)
N5–C24	1.370(4)	C14–C15	1.399(5)	K2–O402	2.819(6)
N6–C24	1.345(4)	C15–C16	1.455(5)	K3–O201	2.757(3)
N6–C25	1.335(4)	C17–C18	1.439(5)	K3–O202	2.693(3)
N7–C25	1.377(4)	C18–C19	1.407(5)	K3–O301	2.659(7)
N7–C32	1.367(4)	C18–C23	1.402(5)	K3–O302	2.967(4)

**Table 3.** Selected bond angles (°) for [K<sub>2</sub>(DME)<sub>4</sub>]PcMg(OH) (1)

O1–Mg1–N1	114.73(11)	N8–C1–C2	122.3(3)	N5–C17–C18	109.3(3)
O1–Mg1–N3	106.66(11)	C1–C2–C3	133.3(3)	N4–C17–C18	123.3(3)
N1–Mg1–N3	85.81(11)	C1–C2–C7	105.4(3)	C17–C18–C19	133.3(4)
O1–Mg1–N5	99.06(11)	C3–C2–C7	121.1(3)	C17–C18–C23	106.8(3)
N1–Mg1–N5	146.21(12)	C2–C3–C4	118.0(3)	C19–C18–C23	119.9(4)
N3–Mg1–N5	85.05(12)	C3–C4–C5	120.6(3)	C18–C19–C20	117.8(4)
O1–Mg1–N7	106.00(11)	C4–C5–C6	122.3(3)	C19–C20–C21	122.0(4)
N1–Mg1–N7	85.01(11)	C5–C6–C7	117.4(3)	C20–C21–C22	121.0(4)
N3–Mg1–N7	146.98(12)	C2–C7–C6	120.4(3)	C21–C22–C23	118.0(4)
N5–Mg1–N7	85.19(11)	C2–C7–C8	107.6(3)	C18–C23–C22	121.3(3)
Mg1–O1–K3	107.90(10)	C6–C7–C8	131.9(3)	C18–C23–C24	106.4(3)
Mg1–O1–K2	116.75(10)	C7–C8–N1	108.5(3)	C22–C23–C24	132.3(4)
K3–O1–K2	95.91(8)	C7–C8–N2	123.2(3)	C23–C24–N5	109.0(3)
Mg1–N1–C1	126.1(2)	N1–C8–N2	128.2(3)	C23–C24–N6	123.0(3)
Mg1–N1–C8	124.8(2)	N3–C9–N2	128.3(3)	N5–C24–N6	127.9(3)
C1–N1–C8	108.6(3)	N3–C9–C10	108.9(3)	N7–C25–N6	127.7(3)
C8–N2–C9	123.2(3)	N2–C9–C10	122.7(3)	N7–C25–C26	109.1(3)
Mg1–N3–C9	125.4(2)	C9–C10–C11	132.9(4)	N6–C25–C26	123.1(3)

(Continued)

Table 3. (Continued)

Mg1–N3–C16	125.7(2)	C9–C10–C15	106.8(3)	C25–C26–C27	132.3(3)
C9–N3–C16	108.7(3)	C11–C10–C15	120.3(4)	C25–C26–C31	106.7(3)
C16–N4–C17	122.8(3)	C10–C11–C12	117.8(5)	C27–C26–C31	121.0(3)
Mg1–N5–C17	124.0(2)	C11–C12–C13	121.5(4)	C26–C27–C28	117.9(3)
Mg1–N5–C24	123.3(2)	C12–C13–C14	121.1(4)	C27–C28–C29	121.4(3)
C17–N5–C24	108.4(3)	C13–C14–C15	118.0(5)	C28–C29–C30	121.3(3)
C24–N6–C25	123.1(3)	C14–C15–C10	121.2(4)	C29–C30–C31	117.9(3)
Mg1–N7–C25	123.6(2)	C14–C15–C16	132.2(4)	C26–C31–C30	120.6(3)
Mg1–N7–C32	125.4(2)	C10–C15–C16	106.5(3)	C26–C31–C32	106.2(3)
C25–N7–C32	108.7(3)	C15–C16–N3	109.0(3)	C30–C31–C32	133.2(3)
C1–N8–C32	122.7(3)	C15–C16–N4	122.7(3)	C31–C32–N7	109.4(3)
N1–C1–N8	127.9(3)	N3–C16–N4	128.2(3)	C31–C32–N8	122.8(3)
N1–C1–C2	109.8(3)	N5–C17–N4	127.4(3)	N7–C32–N8	127.9(3)

using CRYSTALS [42]. The hydroxide hydrogen atom was located on an electron difference map and linked to its respective oxygen atom using a riding model during refinement. All other hydrogen atoms were placed in idealized geometric positions and linked to their respective carbon atoms using a riding model during refinement. The isotropic temperature factor of each hydrogen atom was initially set to 1.2 times that of the atom it is bonded to and then the temperature factors of groups of similar hydrogen atoms were linked during refinement. DME molecules were disordered and modeled accordingly (see CIF file for details). Crystal structure diagrams were generated using ORTEP-3 for Windows (v. 2.02) [43] and rendered using POV-Ray (v. 3.6.1c) [44].

### Computational methods

Geometry optimizations were performed using the Gaussian 09 program (Revision B.01) [45], the B3LYP functional [46], and the 6–31G\* basis set [47, 48].

## CONCLUSION

The reduction of MgPc with  $KC_8$  in DME and trace moisture or oxygen generates  $[K_2(DME)_4]PcMg(OH)$  containing a singly reduced  $Pc^{3-}$  ligand. The -3 charge of the Pc ligand was confirmed by absorption spectroscopy. This is only the second structurally characterized mono-reduced MPc complex reported in the literature. Unlike the structurally characterized, doubly reduced MPc complexes, which exhibit bond-length alternation within the Pc ligand [20, 21], bond-length alternation is not observed in  $[K_2(DME)_4]PcMg(OH)$ . While both  $Pc^{3-}$  and  $Pc^{4-}$  complexes

have now been structurally characterized, isolating  $Pc^{5-}$  and  $Pc^{6-}$  complexes, which are presumably exceedingly air- and moisture-sensitive, remains a challenge for future research.

### Acknowledgements

We are grateful to the Natural Sciences and Engineering Research Council of Canada for a research grant (DBL) and an Alexander Graham Bell Canada Graduate Scholarship-D (EWYW), Simon Fraser University for funding, and Compute Canada and WestGrid for providing computational resources. We thank Dr. Michael J. Katz for assistance with X-ray crystallography and Professor Tim Storr for assistance with DFT calculations.

We are grateful to Dr. Jeanette A. Krause and the SCrALS program (Lawrence Berkeley National Laboratory) for the X-ray crystallographic data collection of **1**. The ALS is supported by the US Department of Energy, Office of Energy Sciences Materials Sciences Division, under contract DE-AC02-05CH11231.

### Supporting information

Atomic coordinates of the DFT-optimized structure of **1** are given in the supplementary material. This material is available free of charge via the Internet at <http://www.worldscinet.com/jpp/jpp.shtml>.

Crystallographic data have been deposited at the Cambridge Crystallographic Data Centre (CCDC) under number CCDC-851775 (**1**). Copies can be obtained on request, free of charge, via [www.ccdc.cam.ac.uk/data\\_request/cif](http://www.ccdc.cam.ac.uk/data_request/cif) or from the Cambridge Crystallographic Data Centre, 12 Union Road, Cambridge CB2 1EZ, UK (fax: +44 1223-336-033 or email: [deposit@ccdc.cam.ac.uk](mailto:deposit@ccdc.cam.ac.uk)).

## REFERENCES

- Lever ABP. *J. Porphyrins Phthalocyanines* 1999; **3**: 488–499.
- Mack J and Kobayashi N. *Chem. Rev.* 2011; **111**: 281–321.
- Mack J and Stillman MJ. *Coord. Chem. Rev.* 2001; **219**: 993–1032.
- Stillman MJ. *J. Porphyrins Phthalocyanines* 2000; **4**: 374–376.
- Nyokong T and Isago H. *J. Porphyrins Phthalocyanines* 2004; **8**: 1083–1090.
- McKeown NB. *Phthalocyanine Materials: Synthesis, Structure, and Function*; Cambridge University Press: Cambridge, 1998.
- The Porphyrin Handbook*, Vol. 15–20, Kadish KM, Smith KM and Guillard R. (Eds.) Academic Press: San Diego, 2000.
- Phthalocyanines: Properties and Applications*, Vol. 1–4, Leznoff CC and Lever ABP. (Eds.) VCH Publishers, Inc.: New York, 1989.
- Clack DW and Yandle JR. *Inorg. Chem.* 1972; **11**: 1738–1742.
- Shablya AV and Terenin AN. *Opt Spektrosk.* 1960; **9**: 533–535.
- Linder RE, Rowlands JR and Hush NS. *Mol. Phys.* 1971; **21**: 417–437.
- Mack J, Kirkby S, Ough EA and Stillman MJ. *Inorg. Chem.* 1992; **31**: 1717–1719.
- Louati A, Elmeray M, Andre JJ, Simon J, Kadish KM, Gross M and Giraudeau A. *Inorg. Chem.* 1985; **24**: 1175–1179.
- Mack J and Stillman MJ. *Inorg. Chem.* 1997; **36**: 413–425.
- Golovin MN, Seymour P, Jayaraj K, Fu YS and Lever ABP. *Inorg. Chem.* 1990; **29**: 1719–1727.
- Keizer SP, Mack J, Bench BA, Gorun SM and Stillman MJ. *J. Am. Chem. Soc.* 2003; **125**: 7067–7085.
- Mack J and Stillman MJ. *J. Am. Chem. Soc.* 1994; **116**: 1292–1304.
- Cissell JA, Vaid TP and Rheingold AL. *Inorg. Chem.* 2006; **45**: 2367–2369.
- Deng X, Porter WW and Vaid TP. *Polyhedron* 2005; **24**: 3004–3011.
- Cissell JA, Vaid TP, DiPasquale AG and Rheingold AL. *Inorg. Chem.* 2007; **46**: 7713–7715.
- Wong EWY, Walsby CJ, Storr T and Leznoff DB. *Inorg. Chem.* 2010; **49**: 3343–3350.
- Lever ABP and Wilshire JP. *Inorg. Chem.* 1978; **17**: 1145–1151.
- Rollmann LD and Iwamoto RT. *J. Am. Chem. Soc.* 1968; **90**: 1455–1463.
- Nevin WA, Hempstead MR, Liu W, Leznoff CC and Lever ABP. *Inorg. Chem.* 1987; **26**: 570–577.
- Guillard R, Dormond A, Belkalem M, Anderson JE, Liu YH and Kadish KM. *Inorg. Chem.* 1987; **26**: 1410–1414.
- Mack J and Stillman MJ. In *Phthalocyanines: Spectroscopic and Electrochemical Characterization*, Vol. 16, Kadish KM, Smith KM and Guillard R (Eds.) Academic Press: San Diego, 2003; pp 69.
- Taube R. *Pure Appl. Chem.* 1974; **38**: 427–438.
- Tahiri M, Doppelt P, Fischer J and Weiss R. *Inorg. Chim. Acta* 1987; **127**: L1–L3.
- Janczak J and Kubiak R. *Polyhedron* 2001; **20**: 2901–2909.
- Bouwkamp MW, Lobkovsky E and Chirik PJ. *Inorg. Chem.* 2005; **45**: 2–4.
- Fortney CF, Serli B, Zangrando E, Geib SJ and Shepherd RE. *Cambridge Structural Database Code FUQHOP*, 2009.
- Kam KC, Young KLM and Cheetham AK. *Cryst. Growth Des.* 2007; **7**: 1522–1532.
- Abrahams I, Lazell M, Motevalli M, Simon CK and Sullivan AC. *Khim. Geterotsiklicheskikh Soedin.* 1999: 1085–1097.
- Engel MK. In *The Porphyrin Handbook*, Vol. 20, Kadish KM, Smith KM and Guillard R. (Eds.) Academic Press: San Diego, 2003.
- Mizuguchi J. *J. Phys. Chem. A* 2001; **105**: 1121–1124.
- Guzei IA, McGaff RW and Kieler HM. *Acta Crystallogr.* 2005; **C61**: m472–m475.
- Janczak J and Idemori YM. *Acta Crystallogr.* 2002; **C58**: m549–m550.
- Stillman MJ and Nyokong T. In *Phthalocyanines: Properties and Applications*, Vol. 1, Leznoff CC and Lever ABP. (Eds.) Wiley: New York, 1989; pp 133–289.
- Stillman MJ. In *Phthalocyanines: Properties and Applications*, Vol. 3, Leznoff CC and Lever ABP. (Eds.) VCH: New York, 1993; p 227.
- Schwindt MA, Lejon T and Hegedus LS. *Organometallics* 1990; **9**: 2814–2819.
- Altomare A, Cascarano G, Giacovazzo C and Guagliardi A. *J. Appl. Crystallogr.* 1993; **26**: 343–350.
- Betteridge PW, Carruthers JR, Cooper RI, Prout K and Watkin DJ. *J. Appl. Crystallogr.* 2003; **36**: 1487.
- Farrugia LJ. *J. Appl. Crystallogr.* 1997; **30**: 565.
- Persistence of Vision (TM) Raytracer, Version 3.6.1*; Persistence of Vision Pty. Ltd.: Williamstown, Victoria, Australia, 2004.
- Frisch MJ, Trucks GW, Schlegel HB, Scuseria GE, Robb MA, Cheeseman JR, Scalmani G, Barone V, Mennucci B, Petersson GA, Nakatsuji H, Caricato M, Li X, Hratchian HP, Izmaylov AF, Bloino J, Zheng G, Sonnenberg JL, Hada M, Ehara M, Toyota K, Fukuda R, Hasegawa J, Ishida M, Nakajima T, Honda Y, Kitao O, Nakai H, Vreven T, Montgomery JA, Peralta JE, Ogliaro F, Bearpark M, Heyd JJ, Brothers E, Kudin KN, Staroverov VN, Keith T,

Kobayashi R, Normand J, Raghavachari K, Rendell A, Burant JC, Iyengar SS, Tomasi J, Cossi M, Rega N, Millam JM, Klene M, Knox JE, Cross JB, Bakken V, Adamo C, Jaramillo J, Gomperts R, Stratmann RE, Yazyev O, Austin AJ, Cammi R, Pomelli C, Ochterski JW, Martin RL, Morokuma K, Zakrzewski VG, Voth GA, Salvador P, Dannenberg JJ, Dapprich S, Daniels AD, Farkas O, Foresman JB, Ortiz

JV, Cioslowski J and Fox DJ. *Gaussian 09, Revision B.01*; Gaussian, Inc.: Wallingford CT, 2010.

46. Becke AD. *J. Chem. Phys.* 1993; **98**: 5648–5652.
47. Petersson GA and Al-Laham MA. *J. Chem. Phys.* 1991; **94**: 6081.
48. Petersson GA, Bennett A, Tensfeldt TG, Al-Laham MA, Shirley WA and Mantzaris J. *J. Chem. Phys.* 1988; **89**: 2193.